

Hydrogen bonding and dynamics of methanol by high-pressure diamond-anvil cell NMR

Takuo Okuchi,^{a)} George D. Cody, Ho-kwang Mao, and Russell J. Hemley
Geophysical Laboratory, Carnegie Institution of Washington, Washington, DC 20015

(Received 15 March 2005; accepted 6 May 2005; published online 1 July 2005)

Liquid methanol at densities up to $\rho/\rho_0=1.7$ was studied by NMR in a specially designed diamond-anvil cell. Methyl and hydroxyl resonances have been separately observed at pressures to 43 kbars which exceeds equilibrium freezing pressure of methanol. The chemical shift difference between methyl and hydroxyl protons increases nonlinearly with increasing density, indicating a noticeable decrease in hydrogen bond length. The analyses of spin-lattice relaxation rates of both hydroxyl and methyl protons indicate that compression enhances intermolecular proton exchange and selectively reduces motion of the hydroxyl protons. Collectively these observations reveal that hydrogen bonding interaction in liquid methanol noticeably increases with compression, inhibiting the liquid-solid transition even above the freezing pressure. © 2005 American Institute of Physics.
[DOI: 10.1063/1.1944732]

I. INTRODUCTION

Methanol has been used as a model system for studies of hydrogen bonding in the liquid state. A useful approach to such studies is to enhance intermolecular interactions via compression, forcing the molecules to interatomic distances not otherwise accessible. Early on, Bridgman reported a disparity in a pair of density measurements made at pressures above 24.5 kbars.¹ He concluded that such a disparity was evidence of a metastable liquid phase. Later Piermarini *et al.*² observed that liquid methanol exhibited zero shear strength up to 86 kbars, which far exceeded the freezing pressure of 35 kbars.²⁻⁴ They also observed that a mixture of 4:1 methanol:ethanol exhibited zero shear strength to 104 kbars; this solution has subsequently become a common hydrostatic pressure medium for high-pressure experiments. The viscosities of methanol and the 4:1 mixture were liquid-like up to at least 84 and 70 kbars, respectively.^{5,6} The glass transition pressure was found to be 105 kbars and the glassy methanol did not devitrify up to at least 330 kbars.⁷

Methanol has also been studied spectroscopically by nuclear magnetic resonance (NMR) at pressures up to 3.5 kbars (Refs. 8-11) and by Raman scattering up to 20 kbars.¹² The NMR chemical shift reflects the electron current density surrounding the resonant nuclei; hence this shift of hydroxyl protons δ_H is exquisitely sensitive to the hydrogen bond length.^{13,14} In the case of methanol, δ_H has been referenced to methyl protons δ_M in order to eliminate the effect of possible bulk susceptibility change at pressures. Previous measurements demonstrated that the difference of $\delta_H - \delta_M$ slightly increased with pressure.⁸⁻¹⁰ It was also shown that for dilute methanol in a nonpolar solvent, the $\delta_H - \delta_M$ increased faster than in the case of pure methanol.¹¹

This difference was ascribed to enhanced oligomerization via hydrogen bonding of dilute methanol molecules, a trend favored by negative volume change associated with the hydrogen bonding formation. An alternative interpretation has emerged from the analysis of OH band profiles measured by Raman scattering.¹² With these data it was argued that at pressures between 7 and 20 kbars, the oligomerization did not proceed anymore. Unfortunately, at higher pressures the OH band became too weak to resolve.³ Thus, Raman scattering failed to provide any information on the state of hydrogen bonding in liquid methanol at pressures above 20 kbars, where the most puzzling behavior has been observed. Obviously, NMR spectroscopy at such pressure regime will be extremely useful to address the problem of methanol. We, therefore, have conducted NMR of liquid methanol up to 45 kbars using a diamond-anvil cell (DAC).

II. EXPERIMENT

The use of DACs for NMR has a history of challenges.¹⁵ High-resolution NMR in DACs has been intrinsically difficult¹⁶ and only one spectrum of methanol at 11 kbars, was reported so far.¹⁷ Our data are acquired up to four times this pressure with the aid of three technical breakthroughs: a nonmagnetic DAC capable of generating large force while in the field of a superconducting magnet,¹⁸ a new rf probe design for DAC-NMR with improved sensitivity,¹⁹ and a metallic gasket with magnetic susceptibility matching to the sample.²⁰ We have successfully obtained not only NMR spectra at high pressures, but also derived relaxation times of each resonance from time evolution of these spectra.

The use of large 1.0-mm culet anvils ensures a sufficiently large number of protons in the sample to induce detectible NMR signal. Gaskets were preindented at 2-5 GPa before drilling, where the diameters of sample holes are 0.6 mm for measurements at 14 kbars, 0.4 mm at 27 kbars, and 0.3 mm at 45 kbars. Anhydrous methanol²¹ was loaded into the sample hole in a dry glove box filled with argon.

^{a)}Author to whom correspondence should be addressed. Present address: Graduate School of Environmental Studies, Nagoya University, Furo-cho, Chikusa, Nagoya 464-8601, Japan. Electronic mail: okuchi@eps.nagoya-u.ac.jp

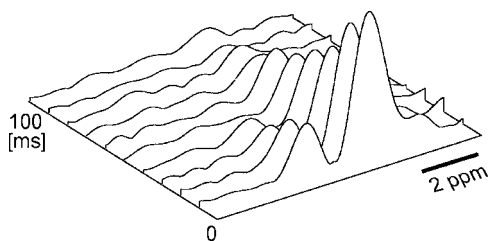


FIG. 1. Time evolution of ^1H transverse magnetization observed at 2.7 GPa.

Pressure was determined using the ruby scale before and after each data acquisition. The reproducibility was better than 1 kbars, and the accuracy of the pressure scale was 1.5 kbars up to the highest pressure. The NMR spectra at 200.1-MHz Larmor frequency were obtained by Fourier transform of the entire spin echoes. This procedure ensures to give pure absorption spectra²² circumventing the ambiguity associated with phase correction of broadened spectra with low signal-to-noise ratios. The spin-lattice relaxation times (T_1) were obtained by the saturation recovery method with a saturating comb sequence.²³ This sequence ensures that observed magnetization has exactly zero value at the beginning of its time evolution. The spin-spin relaxation times (T_2) were obtained with the Carr–Purcell–Meiboom–Gill sequence.²⁴ In both cases a simple exponential decay of each peak was observed within the experimental uncertainty. Figure 1 shows an example of a decaying spectrum at 27 kbars from which the T_2 of hydroxyl and methyl resonances were separately determined. All spectra were obtained at room temperature (21 °C).

III. CHEMICAL SHIFT ANALYSIS

The NMR spectra of liquid methanol obtained at various pressures are shown in Fig. 2(a). The methyl resonance was chosen as the internal reference, defined as 0 ppm. With in-

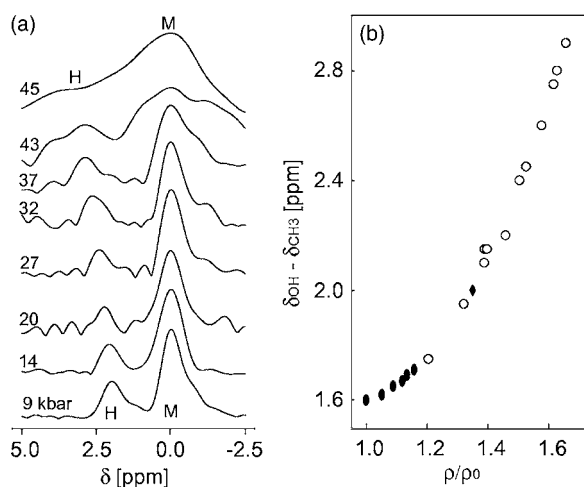


FIG. 2. (a) ^1H NMR spectra of methanol. Pressures are shown on the left. The hydroxyl (H) resonance is on the left and the methyl (M) resonance is on the right. The M resonance is aligned as the internal reference. (b) The chemical shift difference between H and M resonances as a function of normalized density ρ/ρ_0 where ρ_0 is the density of liquid methanol at ambient pressure. Filled circles, capillary NMR results at 24 °C (Ref. 10) for which small temperature corrections were applied; Filled diamond, previous DAC-NMR result (see Ref. 17); Open circles, present DAC-NMR results.

creasing pressure molecular motion is more restricted, yielding a longer molecular correlation time τ_C , hence shorter T_1 and T_2 . Fortunately, the shorter T_1 's enabled us to accumulate more transients in a given time, enhancing the weak signal derived from the smaller number of protons. Unfortunately, the shorter T_2 's gave rise to significant line broadening that ultimately hindered resolution of the two resonances at 45 kbars. The estimated uncertainty of the chemical shift was less than 0.1 ppm at 35 kbars and 0.15 ppm at higher pressure. This was sufficient to quantify the change in $\delta_H - \delta_M$, which increased from 1.6 to 2.9 ppm. Figure 2(b) presents the $\delta_H - \delta_M$ as a function of normalized density of methanol obtained from its equation of state.⁴ Note that our results are in excellent agreement with the previous data obtained using both capillary and DAC apparatuses.^{10,17} This agreement ensures that the NMR signal arises exclusively from within the tiny DAC sample chambers.

The $\delta_H - \delta_M$ grows nonlinearly with increasing density toward the metastable regime. Two different processes may serve to explain this increase. First, the number of hydrogen bonds may increase with increasing pressure.^{10,11} At ambient pressure, a 5.0-ppm increase of $\delta_H - \delta_M$ was observed when the gas transforms to the liquid, which is associated with the formation of hydrogen bonds from free monomers.²⁵ The observed 1.3-ppm increase by compression of the liquid gives a total of 6.3 ppm higher $\delta_H - \delta_M$ for the liquid at 43 kbars than for the gas at ambient pressure. The increase in $\delta_H - \delta_M$ by a factor of 1.26 by compression of the liquid may simply reflect a larger number of hydrogen bonds. X-ray and neutron-diffraction studies demonstrated that liquid methanol has 1.77 ± 0.07 hydrogen bonds per molecule at ambient pressure,^{26,27} thus one might conclude that the methanol at 43 kbars has $1.77 \times 1.26 = 2.2$ hydrogen bonds per molecule.

The problem with this estimate is such a number of hydrogen bonds exceeds the maximum number possible for methanol. Each methanol molecule can donate one hydroxyl proton to form a hydrogen bond, while it can accept two protons with the two lone electron pairs of the oxygen. Since the number of available protons is smaller than the number of proton acceptor sites, the maximum number of hydrogen bonds for methanol is limited by the number of protons. If all available protons form hydrogen bonds, there must be two hydrogen bonds per molecule, one per each molecule by donating its proton and one per each molecule by accepting another proton. It is possible for some molecules to accept two protons simultaneously. However, in this case the exactly same number of molecules has no protons to accept, so that the maximum number of hydrogen bonds does not increase anymore. This limit could only be circumvented if two oxygen simultaneously accept a proton to form two hydrogen bonds, which is energetically unfavorable due to their strong repulsive interaction, and has never been observed in crystalline methanol even in the highest-pressure phase.²⁸ Therefore, formation of new hydrogen bonds in the liquid cannot be the primary reason for the observed increase of $\delta_H - \delta_M$. This is consistent with the Raman-scattering results suggesting the increase in the number of hydrogen bonds stops above 7 kbars.¹²

The accelerative increase of $\delta_H - \delta_M$ even above

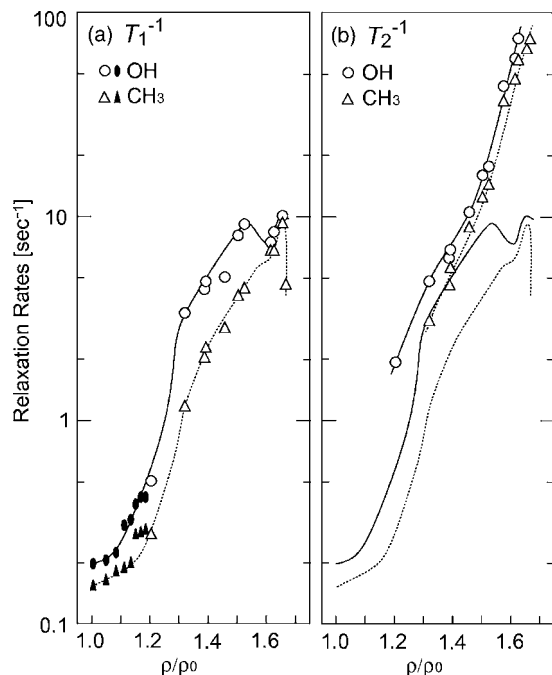


FIG. 3. Spin-lattice (a) and spin-spin (b) relaxation rates. Closed circles, H protons by capillary NMR (Ref. 10); open circles, H protons; closed triangles, M protons by capillary NMR (Ref. 10); open triangles, M protons. The lines are guides to the eye; solid lines, H protons; dotted lines, M protons.

$\rho/\rho_0=1.25$ ($P=7$ kbars) indicates some other change to the hydrogen bonding network. The most likely explanation is that, on average, hydrogen bond length noticeably decreases in this pressure regime. Note that a shortening of bond length is not always necessary to reduce the volume of disordered liquid structures. This is because, without periodic lattice constraint, intermolecular bond angles are often more easily modified to reduce the volume than the bond length. As a first-order approximation, we assume a linear relationship between $\delta_H - \delta_M$ and hydrogen bond length. The proportional factor is estimated to be 0.3 ppm/0.01 Å shortening of the O–O distance, which was evaluated at ambient pressure by a linear fitting between δ_H and O–O distances in various hydrogen bonding compounds with known crystal structures.¹³ The observed 1.3-ppm increase of $\delta_H - \delta_M$ can, therefore, be accounted for by the reduction of the O–O distance by 0.04 Å. The diffraction studies demonstrated that liquid methanol at ambient pressure had the averaged O–O distance of 2.80 ± 0.14 Å (Ref. 26) or 2.72 ± 0.13 Å.²⁹ As O–O distances in the high-pressure phase of crystalline methanol are distributed between 2.6 and 2.8 Å at 40 kbars,²⁸ the averaged O–O distance of liquid methanol at 43 kbars, 2.76 ± 0.14 Å, or 2.68 ± 0.13 Å is consistent with the solid crystalline structure at comparable pressure. The observed decrease of OH Raman frequencies is also qualitatively consistent with such shortening of hydrogen bonds.¹²

IV. RELAXATION RATE ANALYSIS

The observed relaxation rates of hydroxyl protons (T_{1H}^{-1} and T_{2H}^{-1}) and methyl protons (T_{1M}^{-1} and T_{2M}^{-1}) are shown in Fig. 3 as a function of normalized density. Estimated errors

in T_1 results are $\pm 5\%$ to $\rho/\rho_0=1.4$ ($P=14$ kbars) and $\pm 15\%$ at the highest density. Estimated errors in T_2 results are $\pm 5\%$ to $\rho/\rho_0=1.4$ but increase to $\pm 30\%$ at the highest density because their smaller values at higher pressures yield much smaller numbers of echo trains, especially for hydroxyl protons (Fig. 1). Note that our T_1 's at $\rho/\rho_0=1.19$ ($P=4$ kbars) are in excellent agreement with the capillary NMR results at $\rho/\rho_0=1.17$ ($P=3.5$ kbars) for both hydroxyl and methyl protons. No T_2 results for these specific proton species at pressures comparable to our study have been reported.

As previously noted, both T_1^{-1} and T_2^{-1} increase due to the increase of τ_C with increasing density. The maximum of T_1^{-1} at $\rho/\rho_0=1.66$ (43 kbars) is indicative of τ_C^{-1} being equal to ω_0 , as observed at similar pressure by bulk relaxation measurements of methanol-ethanol mixture.¹⁵ At lower density the extreme narrowing condition $\omega_0\tau_C \ll 1$ should be satisfied, where the relaxation rates by dipole-dipole interactions, $1/T_{1d}$ and $1/T_{2d}$, are

$$T_{1dH}^{-1} = T_{2dH}^{-1} = f_H(r_{1H}, r_{2H} \dots r_{nH})\tau_{CH}, \quad (1)$$

$$T_{1dM}^{-1} = T_{2dM}^{-1} = f_M(r_{1M}, r_{2M} \dots r_{nM})\tau_{CM},$$

where r_n is the distance to the n th interacting spin from the relaxing spin.³⁰ Note that the M protons have additional internal freedom of rotation which may separate τ_{CH} and τ_{CM} at pressures. The two correlation times are therefore distinguished. In order to describe the spin relaxation in liquid methanol, we need also to introduce the exchange probability W of spin state between H and M protons through their scalar interaction, or electron-coupled spin-spin interaction,³¹

$$W = \frac{4\pi^2 J^2 \tau_e}{\{1 + 4\pi^2 (\delta_H - \delta_M)^2 \tau_e^2\}}. \quad (2)$$

Here J is the scalar coupling constant between H and M protons in hertz, τ_e is the average lifetime for intermolecular proton exchange in seconds, and $\delta_H - \delta_M$ is the chemical shift difference between H and M protons in hertz. Phenomenologically, the relaxation of longitudinal magnetizations M_H and M_M follows as:³¹

$$\begin{aligned} \frac{dM_H(t)}{dt} &= -(3W + T_{1dH}^{-1})(M_H - M_{H0}) + W(M_M - M_{M0}), \\ \frac{dM_M(t)}{dt} &= 3W(M_H - M_{H0}) - (W + T_{1dM}^{-1})(M_M - M_{M0}), \end{aligned} \quad (3)$$

where M_{H0} and M_{M0} are the equilibrium magnetizations of H and M protons. The solution of the simultaneous differential equations is a linear combination of two exponentials, $\exp(W_a t)$ and $\exp(W_b t)$, where W_a and W_b are eigenvalues of the matrix consisting of four coefficients of the equations,

$$\begin{aligned} W_a &= -(T_{1dH}^{-1} + T_{1dM}^{-1} + 2W) - (D^2/4 + DW + 4W^2)^{1/2}, \\ W_b &= -(T_{1dH}^{-1} + T_{1dM}^{-1} + 2W) + (D^2/4 + DW + 4W^2)^{1/2}, \end{aligned} \quad (4)$$

where D is the difference between H and M dipolar relaxation rates ($=T_{1dH}^{-1} - T_{1dM}^{-1}$). The initial condition of saturation recovery method is $M_H(0) = M_M(0) = 0$. We also have the relation $3M_{H0} = M_{M0}$ because the methyl protons are three times more abundant than the hydroxyl protons. Using these

conditions and assuming $D \gg W$, the solution can be simplified to,

$$M_H(t) \approx M_{H0}\{1 - \exp(W_a t)\}, \quad (5)$$

$$M_M(t) \approx M_{M0}\{1 - \exp(W_b t)\}.$$

The spin-lattice relaxation rates are

$$T_{1H}^{-1} = -W_a \approx T_{1dH}^{-1} + 3W, \quad (6)$$

$$T_{1M}^{-1} = -W_b \approx T_{1dM}^{-1} + W.$$

Accordingly, when the scalar relaxation W is substantial, it will serve to increase T_{1H}^{-1} three times greater than T_{1M}^{-1} . The increasing separation between T_{1H}^{-1} and T_{1M}^{-1} at around $\rho/\rho_0 = 1.3$ demonstrates such an effect [Fig. 3(a)]. The τ_e at ambient pressure is ~ 0.1 s for pure methanol, yielding a negligible value of W on the order of 10^{-3} s^{-1} .³² This is a much smaller value than D so that the assumption $D \gg W$ is well satisfied. With increasing density, τ_e is expected to decrease because the observed shortening of hydrogen bonds will facilitate proton exchange. Equation (2) predicts that with decreasing τ_e , W increases, reaching a maximum,

$$W_{\max} = \frac{\pi J^2}{\delta_H - \delta_M}, \quad (7)$$

where τ_e^{-1} passes through the $2\pi(\delta_H - \delta_M)$, and decreases again. This entire evolution of W was already observed under ambient pressure by adjusting the acidity of methanolic solutions to control τ_e .³² In our case the same evolution has been observed by changing the density; τ_e has decreased to 0.4 ms when $W = W_{\max}$. This τ_e is more than two orders of magnitude smaller than its value at ambient pressure. With further increase of density, τ_e becomes even smaller.

The effect of evolution of W is more obviously seen in the difference between two spin-lattice relaxation rates,

$$\Delta R_1 = T_{1H}^{-1} - T_{1M}^{-1} \approx D + 2W. \quad (8)$$

Figure 4(a) presents the observed ΔR_1 with circles. An abrupt increase of ΔR_1 is observed at $\rho/\rho_0 = 1.3$ ($P = 9$ kbars). Since we do not expect any reason for an abrupt increase of D which only involves dipolar interactions in Eq. (1), the $2W$ should have increased and reached a maximum around this density. Using $J = 5.2$ Hz at ambient pressure,³¹ Eq. (7) gives $2W_{\max} = 0.5 \text{ s}^{-1}$ which is shown by an arrow in Fig. 4(a). The arrow is somewhat shorter than the observed trend which might be explained by an increase of J induced by a possible change of electron density around the hydroxyl protons at pressure.

In the lowest- and highest-density regimes in Fig. 4(a), W is negligible so that the observed spin-lattice relaxation rates, T_{1H}^{-1} and T_{1M}^{-1} , are equal with the dipolar relaxation rates, T_{1dH}^{-1} and T_{1dM}^{-1} [Eq. (6)]. Thus Eq. (1) yields the ratio of the H and M spin-lattice relaxation rates,

$$\frac{T_{1M}}{T_{1H}} = \frac{T_{1dM}}{T_{1dH}} = \frac{f_H}{f_M} \cdot \frac{\tau_{CH}}{\tau_{CM}}.$$

This ratio is presented in Fig. 4(b). The term f_H/f_M is likely to be insensitive to the pressure because the dipolar interaction works most efficiently within the molecules which maintain a solid framework at the pressures in this study.

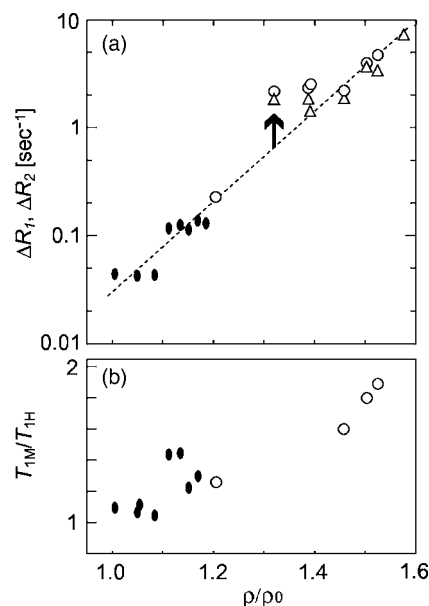


FIG. 4. (a) The difference between H and M spin-lattice relaxation rates. Circles, $\Delta R_1 = T_{1H}^{-1} - T_{1M}^{-1}$; Triangles, $\Delta R_2 = T_{2H}^{-1} - T_{2M}^{-1}$. The broken line shows the change of D that is approximated by a linear fitting to ΔR_1 at $\rho/\rho_0 < 1.2$ and at $\rho/\rho_0 > 1.5$ where the contribution of W is negligible. Apparent deviations of ΔR_1 and ΔR_2 at $1.3 < \rho/\rho_0 < 1.4$ from the broken line reflect the evolution of W with increasing density. The arrow shows $2W_{\max}$ calculated from Eq. (7) with the value of J at ambient pressure. (b) The ratio of H and M spin-lattice relaxation rates. The results affected by the contribution of W at $1.3 < \rho/\rho_0 < 1.4$ are not shown. The increase of this ratio indicates a selective reduction of motion in hydroxyl protons. In both (a) and (b), the filled symbols show capillary NMR results (see Ref. 10) and the open symbols show the present DAC-NMR results.

Accordingly, the τ_{CH}/τ_{CM} must have increased by compression, demonstrating a selective reduction of motion of hydroxyl protons. The transport properties of alcohols at high pressures are, therefore, beyond the description provided by standard theories that assume spatially rigid molecules, as noted independently by dielectric relaxation experiments at high pressure.³³

So far the observed spin-lattice relaxation rates (T_{1H}^{-1} and T_{1M}^{-1}) are explained by the combination of dipolar and scalar interactions. Next we interpret the observed spin-spin relaxation rates (T_{2H}^{-1} and T_{2M}^{-1}) as being the sum of the same combination. The formulations are³¹

$$T_{2H}^{-1} = T_{2dH}^{-1} + \frac{3}{4}(4\pi^2 J^2 \tau_e + W), \quad (10)$$

$$T_{2M}^{-1} = T_{2dM}^{-1} + \frac{1}{4}(4\pi^2 J^2 \tau_e + W).$$

The difference between H and M relaxation rates is

$$\Delta R_2 = T_{2H}^{-1} - T_{2M}^{-1} = D \frac{1}{2}(4\pi^2 J^2 \tau_e + W). \quad (11)$$

Assuming $\tau_e^{-1} = 2\pi(\delta_H - \delta_M)$ for $W = W_{\max}$,

$$\Delta R_2 = D + \frac{3}{2} \cdot \frac{\pi J^2}{(\delta_H - \delta_M)} = D + \frac{3}{2} W_{\max}. \quad (12)$$

Thus we expect a similar effect of the evolution of scalar relaxation W with decreasing τ_e . Note that the effect of W for ΔR_2 in Eq. (12) is a factor of 3/4 smaller than that for ΔR_1 in Eq. (8). Figure 4(a) presents the observed ΔR_2 with open triangles. At around $\rho/\rho_0 = 1.3$ where $W \sim W_{\max}$, the ΔR_2 positively deviates from D as ΔR_1 does. The deviation of

ΔR_2 is smaller than that of ΔR_1 as expected. With further increase of density, the second term in Eq. (11) becomes smaller so that ΔR_2 is expected to approach to D as ΔR_1 does. This expectation is consistent with the trend observed for ΔR_2 at higher density. However, the larger errors for T_2 measurements at $\rho/\rho_0 > 1.4$ make the trend of ΔR_2 to be much less definitive than the trend observed for ΔR_1 .

From the relaxation rate analyses, it has been shown that both T_1 and T_2 evolutions as a function of density are consistently explained by the combination of dipolar and scalar interactions. These analyses have distinctly shown how dynamics of hydrogen-bonded molecules in the liquid changes with increasing density. At ambient pressure, transport of protons in liquid methanol was simulated by *ab initio* molecular dynamics.³⁴ Such simulation studies at high pressures, as well as more diamond-anvil cell NMR results, are expected to enforce the emerging picture of proton dynamics in hydrogen-bonded liquids at high pressures.

V. CONCLUSIONS

Pressure-induced shortening in hydrogen bond distances, acceleration of proton exchange, and selective reduction of motion of the hydroxyl protons are independently derived from NMR spectra and relaxation rate analyses of liquid methanol at densities to $\rho/\rho_0 \sim 1.7$. These observations are consistent with a noticeable increase in hydrogen bonding interactions as a consequence of extensive compression. Our previous understanding of hydrogen bonding in compressed materials has been primarily derived from structural analysis of H_2O at high pressures. However, as for the disordered structures relevant to the present study, previous analyses at high pressures have failed to directly confirm the shortening of hydrogen bonds. In fact, the first coordination shell of liquid H_2O (Ref. 35) and amorphous H_2O ices³⁶ has been considered to be remaining unperturbed by compression. Instead, extensive deformation in the second coordination shell was observed as the primary structural change for both liquid and amorphous H_2O phases, indicating that O–O–O angles are more easily modified than O–O distances in disordered, hydrogen-bonded molecular systems. The structure of liquid methanol was also studied by diffraction at pressures of 9 kbars,²⁹ which also failed to observe any shortening of the O–O distance. In the present study of liquid methanol, however, we actually observed that the first coordination shell responds directly to the compression. Our different result should arise from the different sensitivity; the chemical shift uncertainty of 0.15 ppm gives a 0.005-Å distance uncertainty, while the diffraction correlation functions of liquid methanol have much larger deviations of 0.14 Å (Ref. 26) or 0.13 Å.²⁹

The observed direct response of the first coordination shell of methanol may provide an explanation of the well-known difficulty in promoting its pressure-driven solidification. Stronger hydrogen bonding at higher pressures in the liquid state may kinetically hinder structural rearrangement. The highly compressed disordered structure of methanol,

therefore, can sustain itself without solidification or devitrification.^{3,7} The unique behavior of compressed methanol is deeply related to the nature of hydrogen bonding at high pressure.

ACKNOWLEDGMENTS

One of the authors (T.O.) was supported by JSPS Postdoctoral Fellowships for Research Abroad. This work was supported by DOE (CDAC), NSF, and NASA.

- ¹P. W. Bridgman, Proc. Am. Acad. Arts Sci. **74**, 403 (1942).
- ²G. J. Piermarini, S. Block, and J. D. Barnett, J. Appl. Phys. **44**, 5377 (1973).
- ³J. F. Mammone, S. K. Sharma, and M. Nicol, J. Phys. Chem. **84**, 3130 (1980).
- ⁴J. M. Brown, L. J. Slutsky, K. A. Nelson, and L.-T. Cheng, Science **241**, 65 (1988).
- ⁵G. J. Piermarini, R. A. Forman, and S. Block, Rev. Sci. Instrum. **49**, 1061 (1978).
- ⁶R. L. Cook, C. A. Herbst, and H. E. J. King, J. Phys. Chem. **97**, 2355 (1993).
- ⁷M. J. P. Brugmans and W. L. Vos, J. Chem. Phys. **103**, 2661 (1995).
- ⁸E. M. Schulman, D. W. Dwyer, and D. C. Doetschman, J. Phys. Chem. **94**, 7308 (1990).
- ⁹S. L. Wallen, B. J. Palmer, B. C. Garrett, and C. R. Yonker, J. Phys. Chem. **100**, 3959 (1996).
- ¹⁰S. Bai and C. R. Yonker, J. Phys. Chem. **102**, 8641 (1998).
- ¹¹C. Czeslik and J. Jonas, Chem. Phys. Lett. **302**, 633 (1999).
- ¹²A. Arencibia, M. Taravillo, F. J. Perez, J. Nunez, and V. G. Baonza, Phys. Rev. Lett. **89**, 195504 (2002).
- ¹³C. M. Rohlfing, L. C. Allen, and R. Ditchfield, J. Chem. Phys. **79**, 4958 (1983).
- ¹⁴B. G. Pfrommer, F. Mauri, and S. G. Louie, J. Am. Chem. Soc. **122**, 123 (2000).
- ¹⁵S.-H. Lee, K. Luszczynski, and R. E. Norberg, Rev. Sci. Instrum. **58**, 415 (1987).
- ¹⁶J. L. Yarger, R. A. Nieman, G. H. Wolf, and R. F. Marzke, J. Magn. Reson., Ser. A **114**, 255 (1995).
- ¹⁷K. E. Halvorson, D. P. Raffaele, G. H. Wolf, and R. F. Marzke, in *Frontiers of High-Pressure Research*, edited by H. D. Hochheimer and R. D. Eppers (Plenum, New York, 1991), p. 217.
- ¹⁸T. Okuchi, Phys. Earth Planet. Inter. **143–144**, 611 (2004).
- ¹⁹T. Okuchi, R. J. Hemley, and H. K. Mao, Rev. Sci. Instrum. **76**, 026111 (2005).
- ²⁰T. Okuchi, R. J. Hemley, and H. K. Mao, in *Advances in High Pressure Technology for Geophysical Applications*, edited by J. Chen, Y. Wang, T. Duffy, G. Shen and L. Dobrzynetskaya (Elsevier, New York, 2005), p. 503.
- ²¹Alfa Aesar, Ward Hill, MA, 41838.
- ²²A. Bax, J. Magn. Reson. (1969–1992) **65**, 142 (1985).
- ²³E. Fukushima and S. B. W. Roeder, *Experimental Pulse NMR: A Nuts and Bolts Approach* (Addison-Wesley, Reading, MA, 1981), p. 174.
- ²⁴S. Meiboom and D. Gill, Rev. Sci. Instrum. **29**, 688 (1958).
- ²⁵M. M. Hoffmann and M. S. Conradi, J. Phys. Chem. **102**, 263 (1998).
- ²⁶A. H. Narten and A. Habenschuss, J. Chem. Phys. **80**, 3387 (1984).
- ²⁷T. Yamaguchi, K. Hikada, and A. K. Soper, Mol. Phys. **97**, 603 (1999).
- ²⁸D. R. Allan, S. J. Clark, M. J. P. Brugmans, G. J. Ackland, and W. L. Vos, Phys. Rev. B **58**, R11809 (1998).
- ²⁹T. Weitkamp, J. Neufeind, H. E. Fischer, and M. D. Zeidler, Mol. Phys. **98**, 125 (2000).
- ³⁰T. C. Farrar and E. D. Becker, *Pulse And Fourier Transform NMR: Introduction to Theory and Methods* (Academic, New York, 1971).
- ³¹M. Cocivera, J. Chem. Phys. **47**, 1112 (1967).
- ³²T. Fukumi, Y. Arata, and S. Fujiwara, J. Chem. Phys. **49**, 4198 (1968).
- ³³O. Mishima and E. Whalley, J. Chem. Phys. **84**, 2795 (1986).
- ³⁴J. A. Morrone and M. E. Tuckerman, J. Chem. Phys. **117**, 4403 (2002).
- ³⁵A. K. Soper and M. A. Ricci, Phys. Rev. Lett. **84**, 2881 (2000).
- ³⁶S. Klotz, G. Hamel, J. S. Loveday, R. J. Nelmes, M. Guthrie, and A. K. Soper, Phys. Rev. Lett. **89**, 285502 (2002).